Effective interatomic interactions and lattice mechanical properties of the NiO crystal for both paramagnetic and antiferromagnetic phases

S. Ghosh and A. N. Basu

Physics Department, Jadavpur University, Calcutta-700032, India

S. Sengupta

Solid State Physics Research Centre, Physics Department, Presidency College, Calcutta-700013, India

The antiferromagnetic oxide crystals behave rather unusually in respect to many physical properties, and the various attempts to understand them in terms of models which satisfactorily describe the simple ionic solids show conspicuous discrepancies between theory and experiment. One of the major difficulties common to all the existing calculations is that it is not possible to give a consistent description of the elastic properties and the dispersion of phonons of such a crystal in the antiferromagnetic phase within the framework of a single model. Moreover, so far, the magnetic and the mechanical properties of these crystals have been studied, one independent of the other. Apart from this difficulty, a simultaneous description of the dielectric properties and the phonon dispersion with the existing models also presents several problems. In a previous work we have suggested a model which is based on a microscopic analysis of the energy expression of an assembly of ions. Assuming a specific form of the superexchange interaction that is suggested by various experimental and theoretical investigations and incorporating the same in the above model, we have been able to reduce significantly the discrepancies mentioned above for the case of NiO crystal. In addition to this, it has also been possible to present a unified description of the magnetic and the mechanical properties of this crystal with a single model. The specific properties that we have attempted to correlate with a single set of model parameters are: the cohesive and the stability properties, the elastic and the dielectric properties, the dispersion relation of phonons and magnons, and the sublattice magnetization properties. We also indicate the rough order of magnitude of the different interactions implied in the model and the relations that they bear to the unusual features of this solid. Some of the limitations of the present model and the directions of further refinement are also discussed.

I. INTRODUCTION

Although the various physical properties of the antiferromagnetic transition-metal oxides receive increasing attention, the theoretical lattice-dynamical studies of them have mainly been concerned with the dispersion of phonons. In order to contribute to a better understanding of these crystals we should attempt to correlate simultaneously the static and the dynamic properties of a typical crystal belonging to the group within a single model, in particular by incorporating the properties characteristic of the group. We have emphasized elsewhere[1-3] the importance of the unified study of the different properties of a crystal including the vibrational ones in the framework of a single model and with a single set of parameters. In fact, for the simple ionic solids such unified studies have firmly established the validity of the phenomenological models. Under suitable approximations it has been possible to derive the values of the parameters of such models directly from the ionic wave functions which describe the lattice-dynamical behavior with fair accuracy.[4,5]

But the situation with the more complex ionic crystals, in particular the transition-metal oxides, is rather unsatisfactory. It is because of the fact that so far there has been no attempt to develop a uni-

fied study similar to what has been done for the alkali-halide crystals. Moreover, there exist systematic discrepancies between the present calculations and experiment that cannot be removed either by increasing the number of parameters or by adjusting the existing ones within reasonable limits. However, until the advent of a first-principles calculation the phenomenological study can be made more meaningful and may help probe the physical processes present in a crystal in two ways. From a microscopic analysis of the problem we may identify the terms that are responsible for the different interactions. But as is well known, such calculations are too difficult to push rigorously to deliver number. Instead we model the different terms at this stage and the complete model is applied to correlate the major aspects of the statics and dynamics of the solid. Again, as it is not possible to include all the relevant properties (either for want of observation for some of them or prohibitive computational difficulties for others), we usually work with a finite number of properties and hence, it is vitally necessary to supplement the model by some microscopic justification as mentioned above. It is needless to mention that such calculations are more advantageous than pure phenomenology in not only projecting the precise limitation of our present understanding but also in indicating the directions of refinement of the model at the microscopic level. In fact, by following the procedure outlined above, we have recently done such a model calculation for the AgCl crystal,[6] where the majority of terms have some *a priori* justification. In this work we attempt such a calculation which will reproduce the broad features of the NiO crystal, a typical antiferromagnetic oxide.

Before we discuss our work let us briefly review the major peculiarities of the antiferromagnetic oxides in light of the investigations already done. The various versions of the shell model have been usually used to fit the lattice dynamics of these oxides. The number of fitting parameters in the models varies between 8 to 16. One difficulty which is common to these calculations for all the oxides is that with reasonable values of parameters they fail to reproduce the lowering of the transverse-optical (TO) branch in the $\langle 111 \rangle$ direction which is quite pronounced compared to non-transition-metal oxides.[7] The discrepancies at the L point reported by various workers are above experiment by about 20% for CoO,[8] 10% for NiO and MnO,[9] and 15% for FeO.[10] The reason for

this discrepancy is attributed to neglect of the quadrupolar distortion of the charge cloud of the positive ion by Haywood.[9]

Kugel *et al.*[10] observe that the quadrupolar deformation probably has to be considered for better agreement of the dispersion of phonons for FeO, in particular the lowering of the TO branch in the $\langle 111 \rangle$ direction. But so far no attempt has been made to include the effect of this deformability on the lattice-mechanical properties. In this context it may be recalled that Kleppmenn *et al.*[11] have shown that the quadrupolar deformation is intimately connected with the d electron, and the metal ions in the oxides with unfilled $3d$ shells appear to be candidates for generating pronounced quadrupolar-charge deformation.

Another common feature for all these oxides is that if one forces the model to simultaneously fit the dispersion of phonons and the dielectric properties, some of the parameters of the shell model assume unphysical values. In order to fit the zone-boundary frequencies, in particular the longitudinal-optical (LO) branch in the $\langle 111 \rangle$ direction without disturbing the fit for dielectric constants, the shell charge of the positive ion assumes a positive value. Even with this unphysical parameter the low-frequency dielectric constant becomes 10% higher than experiment for NiO, to quote a typical discrepancy.[12] Similar discrepancies are noted for others also. However, for a different interpretation of this point we refer to the work of Bilz *et al.*[13] Further, with the same set of parameters, the calculated cohesive energy and the elastic constants show discrepancies generally well outside the range of experimental error.

Apart from the difficulties mentioned above, the problem of reproducing the elastic constants in these models needs special mention. All the transition-metal oxides undergo an antiferromagnetic ordering below the Néel temperature accompanied by a slight distortion of their normal sodium chloride structure. This phase transition does not affect all the properties equally. The most interesting effect from the point of view of the present study is a sudden increase of C_{11} by about 20 to 30% when the temperature is varied across the Néel point. For NiO (Ref. 14) it is seen that C_{11} increases by about 20% in going from the antiferromagnetic to the paramagnetic phase, whereas there is no appreciable change in either C_{12} or C_{44}.

The situation in the case of CoO (Ref. 15) is particularly interesting where we find a small change in the value of C_{12} in addition to a large

change in C_{11}, and C_{44} remains unaffected. For neither of these two oxides has it been possible so far to simultaneously fit both phonon frequencies and the elastic data within the same model and with the same set of parameters. The best-fit parameters obtained from the phonon data give the value of C_{11} which is larger than experiment by about 25% for NiO and 40% for CoO.

In both cases the phonon frequencies and the elastic data refer to the antiferromagnetic phase. This observation clearly indicates that some magnetic interaction not envisioned in any of the present models must be responsible for this difference. This is further strengthened by the fact that for the same crystal, namely CoO, when fit is organized for the same properties in the paramagnetic phase,[8] the maximum discrepancy for C_{11} is less than 3%. For the MnO crystal in the paramagnetic phase this discrepancy is less than 2%. The effect due to slight distortion from the cubic symmetry of these crystals in the antiferromagnetic phase (for NiO, the cell angle changes from 90° to 90°+3.5′), is too small to account for the large discrepancy mentioned above. On the other hand, the high Néel temperatures of NiO and CoO, namely, 523 and 293 K (compare the same for FeO and MnO which are 198 and 116 K), imply strong antiferromagnetic interaction between the ions which, we presume (if properly taken into account), may resolve the incompatibility mentioned above.

In addition to these properties, measurements for several magnetic properties including the spin-wave dispersion relation in the symmetry directions are also available for these oxides. Until now these two aspects, namely, the mechanical and the magnetic properties, have been studied one independent of the other. It appears that an attempt to unify these two aspects will be highly instructive.

In the next section we shall present an energy expression of an assembly of ions based on the microscopic analysis of the problem. Of the terms, we shall especially mention the two types of short-range polarization mechanisms, the quadrupolar distortion polarizability, and shall discuss in particular the term arising out of the superexchange interactions. Further, we shall see that this antiferromagnetic coupling between the ions provides a natural link that unifies the mechanical and magnetic properties. Our choice of the crystal has been motivated by the fact that the nickel oxide is a prototypical fcc antiferromagnet which orders below the Néel temperature in a type-II fcc spin

pattern.[16] Moreover, with the direct-exchange interaction between the nickel ions compared to indirect superexchange being negligible, the type-II magnetic order may be considered as four unconnected interpenetrating simple cubic lattices, and this leads to a considerable simplification.

Further accurate measurements for a large number of properties are available for this crystal. The specific properties that we shall try to correlate are the following: the cohesive energy, the static lattice structure, the phase-transition properties, the second-order elastic constants, the high- and low-frequency dielectric constants, the phonon-dispersion relation in the symmetry direction, the sublattice magnetization properties, and the magnon-dispersion relation. We shall also try to point out the relation between the characteristic features of this crystal and the different interactions together with a rough order of the estimate of their magnitudes.

II. MODEL

A. Effective interaction between the ions via superexchange mechanism

Anderson[17,18] has studied the theory of indirect exhange between the ions having d or f electrons in the presence of a diamagnetic lattice characteristic of the transition-metal oxides. The essential features of the superexchange theory as formulated by Anderson[17] may be briefly described as follows. In a crystal like NiO the influence of the diamagnetic oxygen ion on the d electrons of the neighboring Ni^{2+} ion is considerably large because of strong overlap interaction. The d functions of Ni^{2+} ions are thereby strongly altered, and the final states, Anderson assumes, are closer to the localized Wannier functions obtained from the Bloch wave functions corresponding to the d band of the crystal. And as a result these localized Wannier functions are a better starting point for a perturbation theory rather than the Bloch wave functions. The Hamiltonian for these d electrons in second-quantized notation may be written as

$$H = \sum_{\vec{k},\sigma} \epsilon(\vec{k}) S^*_{\vec{k}\sigma} S_{\vec{k}\sigma} + V_{es} \tag{1a}$$

where $S^*_{\vec{k}\sigma}$ is the creation operator for a d-band electron with spin σ in a Bloch state and $\epsilon(\vec{k})$ is the corresponding energy interpreted here as a

quasiparticle kinetic energy. V_{es} is the electron-electron interaction term. Bloch wave function diagonalizes the first term in (1a) but the electrostatic energy is strongly nondiagonal. Using the relation[17]

$$S^{*}_{\vec{k}\sigma} = \frac{1}{\sqrt{N}} \sum_{R} e^{-i\vec{k}\cdot\vec{R}} S^{*}(\vec{R},\sigma) ,$$

the same Hamiltonian can be written in terms of localized quasispin states where $S^{*}(\vec{R},\sigma)$ are the creation operators for the electrons in the localized Wannier states at the lattice site R. By dropping the branch index in $S^{*}(\vec{R},\sigma)$ which distinguishes between the five branches of the d orbitals we are, in fact, using the simplified version of only one orbital per spin. The above relation reduces Eq. (1a) to

$$H = \sum_{R,\sigma} \epsilon_0 S^{*}(\vec{R},\sigma) S(\vec{R},\sigma)$$
$$+ \sum_{\vec{R} \neq \vec{R}',\sigma} b(\vec{R}-\vec{R}') S^{*}(\vec{R},\sigma) S(\vec{R},\sigma) + V_{es}$$

$$(1b)$$

In this scheme the major part of V_{es} is diagonal and the only nondiagonal term is the second term, which Anderson calls the transfer integral, between R and R' ions. The parameter b depends upon the overlap of the atomic d functions with the diamagnetic (oxygen) electron functions. The logic in favor of using the localized quasispin as the starting point is the fact that the second term in Eq. (1b) has much weaker nondiagonal elements than the second term in Hamiltonian (1a).

Next, using the second term as a perturbation energy one can immediately write the dominant term in the second-order energy as

$$\Delta E = - \sum_{\vec{R} \neq \vec{R}',\sigma,\sigma'} \frac{|b(\vec{R}-\vec{R}')|^2}{U} S^{*}(\vec{R},\sigma)$$

$$\times S(\vec{R}',\sigma) S^{*}(\vec{R}',\sigma') S(\vec{R},\sigma') ,$$

$$(1c)$$

where U represents the energy due to mutual repulsion of electrons on the same ion. This energy ΔE vanishes unless both $R'\sigma$ and $R\sigma'$ are occupied states [because of the two destruction operators in (1c)]. In the present approximation of one orbital per spin it means that each orbital in d states must be half full.[17] Introducing the spin operators the above expression is simplified, and apart from a constant term is given by

$$\Delta E = \sum_{RR'} \frac{2|b_{R-R'}|^2}{U} \vec{S}_R \cdot \vec{S}_{R'} = \sum_{RR'} J \vec{S}_R \cdot \vec{S}_{R'} . \quad (1d)$$

Here $\vec{S}_R$ denotes the spin value at R site.

Since the introduction of the concept of superexchange there has been intensive investigation (both theoretical and experimental) to estimate the size of this effect.[19] All these lead us to conclude that a pair of metal ions interacting via the common nearest-neighbor oxygen ion can have two different configurations for the NaCl structure. For example, the nearest-neighbor (NN) and the next-nearest-neighbor (NNN) Ni^{2+} ions in the NiO crystal are connected, respectively, by simple 90° and 180° Ni^{2+}-O^{2-}-Ni^{2+} paths involving one intermediate O^{2-} ion. The exchange integral between NN Ni^{2+} ions is usually represented by $J_1^{\pm}$ for a 90° superexchange path. J_1^{+} and J_1^{-} denote integrals corresponding to six NN with parallel spin and antiparallel spin. The 180° superexchange interaction involves the exchange integral J_2.

In order to study the effect of this interaction on the lattice-mechanical properties the dependence of J on the interionic separation (r) is needed, which implies the r dependence of the transfer integral, since U is independent of the lattice spacing. This dependence of J has been thoroughly investigated both theoretically and experimentally.[20] The studies on the pressure dependence of the ordering temperature and the magnetization and effect of thermal expansion behavior of magnetization for various antiferromagnetic materials (including the oxides in question) yield the result

$$- \left[\frac{\partial \ln J}{\partial \ln r} \right]_T \simeq 10 . \quad (2)$$

The dependence is the same for both J_1 and J_2. Again, Johnson et al.[20] have calculated the overlap integral between Ni^{2+} and O^{2-} ions. Their results were later confirmed using more accurate Clementi wave functions by Drickamer.[21] Both obtain the following r dependence of the overlap integral

$$- \left[\frac{\partial \ln S}{\partial \ln r} \right]_T = 2.46 . \quad (3)$$

The latter work further corroborated the same result by measuring the pressure dependence of 10 Dq for MnO and NiO. Since $b_{R-R'} \propto S^r_{R-R'}$ both the relations independently imply

$$b_{R-R'} \propto r_{R-R'}^{-5} . \quad (4)$$

The empirical observations suggest that relation

(4) is not only applicable to the transition-metal oxides but is approximately valid for other systems as well. Using the above result we may write down Eq. (1d) in the following form:

$$\Delta E = \frac{1}{2}\sum_{ik}\sum_{\neq j} k^M r_{ij}^{-5} r_{jk}^{-5} \ , \tag{5}$$

which represents an effective three-body interaction between the ions in a lattice due to the mechanism of superexchange. This interaction is nonvanishing only when j is an oxygen ion and i,k represent two nickel ions, both being nearest neighbors of j. The constant k^M is a joint property of the overlapping ions and the value of this parameter will be different for the two different configurations. Due to thermalization the spin ordering becomes random above the Néel temperature and the energy associated with it given by Eq. (1d) completely vanishes

in the paramagnetic phase even though J remains nonvanishing.

B. Energy expression

The details of the energy expression excluding the superexchange part of it, have been discussed by Ghosh et al.[6] This approach is advantageous in contrast to that of a mechanical model (such as the shell model) in two ways. Firstly, we may dispense with the concepts of the shell charge and the spring constants which are difficult to justify microscopically. Secondly, we can trace the origin of each term occurring in the energy expression from the fundmental considerations. Including the magnetic interaction, the total energy expression in the present model for the antiferromagnetic phase is given as

$$W = \frac{1}{2}\sum_{i,j'}\frac{Z_i Z_j}{r_{ij}} - \sum_i \vec{\mu}_i\cdot\vec{E}_i^m - \frac{1}{2}\sum_i \vec{\mu}_i\cdot\vec{E}_i^\mu + \sum_i \frac{\mu_i^{c^2}}{2\alpha_i} - \sum_i \vec{Q}_i \nabla\vec{E}_i + \frac{1}{2}\sum_{ij} - \frac{c_{ij}}{r_{ij}^6} + \frac{1}{2}\sum_{ij}\phi \left| r_{ij} - \frac{\mu_i^c}{\mu_0} + \frac{\mu_j^c}{\mu_0} \right|$$

$$+ \frac{1}{2}\sum_{ij} b\exp\left[-\frac{r_{ij}}{\rho}\right] + \frac{1}{2}\sum_{ij} b'\exp\left[-\frac{\sqrt{2}r_{ij}}{\rho}\right] + \frac{1}{2}\sum_{jm}\sum_i A(k)\exp\left[-\frac{r_{ij}+r_{im}}{\rho}\right] + \frac{1}{2}\sum_{ik}\sum_j \left[\frac{k^M}{r_{ij}^5 r_{jk}^5}\right] \ , \tag{6}$$

where we have used the same symbols as in Ref. 6. The first four terms represent the pure electrical interaction including the self energy. Here the total dipole moment $\vec{\mu}_i = \vec{\mu}_i^d + \vec{\mu}_i^c$, where $\vec{\mu}_i^d$ and $\vec{\mu}_i^c$ arise because of the first-order exchange interaction and perturbation of the wave function, respectively. The fifth term represents the interaction between the moment developed due to the quadrupolar distortion of the charge cloud and the monopole and dipole fields. The details of the evaluation of this term have been discussed by Ghosh et al.[6,22] The next three terms represent the van der Waals interaction, the change in overlap due to perturbation of the wave function and the usual overlap term.[6] The second-neighbor overlap between the oxygen atoms is given by the ninth term. The tenth term gives the energy due to scalar deformation of the charge cloud, and the last term is due to magnetic interaction. Finally Eq. (6) and the adiabatic condition

$$\frac{\partial W}{\partial \mu_i} = 0 \tag{7}$$

completely describe all the lattice mechanical as well as the magnetic properties of the crystal.

The present model contains eleven adjustable parameters, namely: b and ρ, the short-range overlap parameters; λ, b' and ρ, the second-neighbor overlap parameters; c and ρ' the parameters connected with the deformation dipole $\vec{\mu}_i^d$, arising out of the first-order exchange interaction[6]; μ_{0i} and α, the parameters controlling the dipole moment $\vec{\mu}_i^c$ due to the perturbation of the wave function (only the perturbation of the negative-ion wave functions considered); $A(1)$ and $A(2)$, the scalar-deformation parameters; d_+ the quadrupolar distortion parameter of Ni^{2+} (the quadrupolar distortion of the negative ion is neglected), and k^M, the parameter for the $180°$ $Ni^{2+}-O^{2-}-Ni^{2+}$ configuration superexchange interaction (since in the final calculation we neglect the interaction for the $90°$ configuration). The values of the parameters have been determined by the usual procedure and k^M is obtained from the difference in the values of C_{11} just above and below the Néel temperature. The values of the parameters are quoted in Table I. Since we are not interested in an exact fit of properties and would rather investigate how far it is possible to provide an overall description of different properties in terms of a single set of parameters, the ap-

TABLE I. Value of the parameters.

Parameter	Values
ρ $(10^{-8}$ cm)	0.3150
b $(10^{-9}$ erg)	1.9415
b' $(10^{-9}$ erg)	-2.1980
$A(1)$ $(10^{-6}$ erg)	0.1279
$A(2)$ $(10^{-6}$ erg)	-0.1401
$\mu_{02}(D)$	3.2800
α_2 $(10^{-24}$ cm^3)	4.0586
c (10^{-8})	0.7623
p' $(10^{-8}$ cm)	0.7250
d_+ $(10^{-26}$ dyn cm^4)	-3.3000
k^M $(10^{-90}$ dyn cm^{11})	-0.9770
c_{--} $(10^{-60}$ erg cm^6)^a	65.5
c_{+-} $(10^{-60}$ erg cm^6)^a	8.4

^{a}The van der Waals coefficients are estimated from polarizabilities as given in Ref. 25. c_{++} is neglected being small compared to c_{+-}.

proximations mentioned here will not seriously affect the conclusion.

III. LATTICE STATICS AND ELASTIC PROPERTIES

In order to discuss cohesion and stability we give below the energy per unit cell for the static lattice structure (in the antiferromagnetic phase) for both sodium chloride and hypothetical cesium chloride structures from Eq. (6):

$$\phi_{\text{NaCl}} = \phi_{\text{NaCl}}^N + \phi_{\text{NaCl}}^A , \tag{8}$$

with

$$\phi_{\text{NaCl}}^A = \frac{3k^M(180°)}{r_0^{10}} + \frac{12k^M(90°)}{r_0^{10}} ,$$

where ϕ^N is the nonmagnetic part of the interaction given in Ref. 6 and ϕ^A is the contribution of the superexchange interaction to lattice energy. $k^M(90°)$ and $k^M(180°)$ are the superexchange constants for the two configurations. Similarly, for the hypothetical cesium chloride structure the expression is

$$\phi_{\text{CsCl}} = \phi_{\text{CsCl}}^N + \phi_{\text{CsCl}}^A , \tag{9}$$

with

$$\phi_{\text{CsCl}}^A = \frac{4k^M(180°)}{r_{\text{NN}}^{10}} + \frac{24k^M(90°)}{r_{\text{NN}}^{10}} . \tag{10}$$

In the above expression (10) we have assumed that

the potential parameters remain unaltered. This is not strictly true for the parameter corresponding to the 90° configuration. Since the energy involved is very small and in the final calculation we have neglected it, it is not going to affect the result. The equilibrium nearest-neighbor distance in this structure is obtained by numerically solving the equation

$$\frac{d\phi_{\text{CsCl}}}{dr_{\text{NN}}} = 0 . \tag{11}$$

Using the computed r with and without the magnetic interaction it is found that in both cases the observed structure is predicted. The phase-transition pressure at $T=0$ is obtained in the usual way by equating the Gibbs free energy. The calculated values for the transition pressure and volume together with the contribution from the individual interactions and how they are altered with the change of structure are given Table II. Since in the absence of any observation for the transition pressure the prediction cannot be checked, it may, however, be remarked that the order estimated lies around the range recently reported for other oxides, namely, the CaO crystal which is about 500 to 600 kbar. Since such pressure is experimentally realizable it will be interesting to check the prediction against observation. The implication of the transition pressure without magnetic interaction (see Table II) is that in the paramagnetic phase a higher pressure will be required to bring about the structural change.

Next we calculate the second-order elastic constants. In the following we explicitly write down the contribution to the elastic constants only from the magnetic interaction. Starting from the energy expression (6) and using the theory of homogeneous deformation the expression for the elastic constants for the sodium chloride structure is given by

$$C_{11}^M = \frac{60k^M(180°)}{r_0^{13}} + \frac{140k^M(90°)}{r_0^{13}} , \tag{12a}$$

$$C_{12}^M = \frac{50k^M(90°)}{r_0^{13}} , \tag{12b}$$

$$C_{44}^M = 0 . \tag{12c}$$

The total expression for the elastic constants are given by adding to the above equations the nonmagnetic contributions given in Ref. 6. It is interesting to note that the above equations qualitatively corroborate experimental results. Both the magnetic contributions vanish in the paramagnetic

TABLE II. Cohesion, stability, and phase transition properties.

Structure	Nearest-neighbor distance (Å)	Contribution to cohesive energy by different interactions (erg/mol)						Cohesive energy		Transition pressure (kbar)	Transition volume
		Coulomb	Repulsive	SN overlap	van der Waals	Many body	Mag.	Theor.	Expt.[b]		
NaCl phase	2.0879	−77.240	15.405	−1.120	−1.383	−0.318	−0.186	−64.842	−67.36		
CsCl[a] phase with mag. interaction	2.1570	−75.410	16.494	−2.428	−1.879	−0.385	−0.179	−63.787		383.6	15.12%
CsCl[a] phase without mag. interaction	2.1693	−74.982	15.863	−2.321	−1.816	−0.356		−63.612		494.9	13.66%

[a]Hypothetical structure realizable under high pressure.
[b]Reference 26.

TABLE III. Second-order elastic constants and Debye temperature.

Property	Phase	Expt.[a]	Present calculation	Calculated by Reichardt et al.[b]
$C_{11} \times 10^{-12}$ dyn/cm^2	Antiferro.	3.25	3.2417	3.89
	Paramag.	3.80	3.6517	
C_{12}	Both phases	1.11	1.0060	1.26
C_{44}	Both phases	1.10	1.0333	1.19
Θ_D (K)	Antiferro.	595[c]	508	661
	Paramag.		523	

[a]Reference 14.
[b]Reference 12.
[c]Reference 16.

phase. Experimentally it is found that C_{44} does not change discontinuously either for NiO or CoO. And the change of C_{12} is negligible for NiO but exists for CoO where $k^M(90°)$ is not negligible. Owen et al.[23] theoretically discussed the relative magnitudes of the exchange integrals corresponding to both 90 and 180° configurations for the transition-metal oxides. Their investigations indicate that the contribution corresponding to 90° is vanishingly small compared to that of 180° in the case of NiO. More conservative estimates may be obtained from the work of Hutchings et al.,[16] which implies from the ratio of exchange integrals obtained by fitting of the neutron data that $k^M(90°)$ is approximately twenty times less than $k^M(180°)$. Hence in our final calculation we have totally neglected it. The values obtained for the elastic constants are given in Table III for both phases together with other calculations. Also the Debye temperature at 0 K (Θ_D), evaluated from the elastic constants with and without the superexchange effect, are compared in Table III.
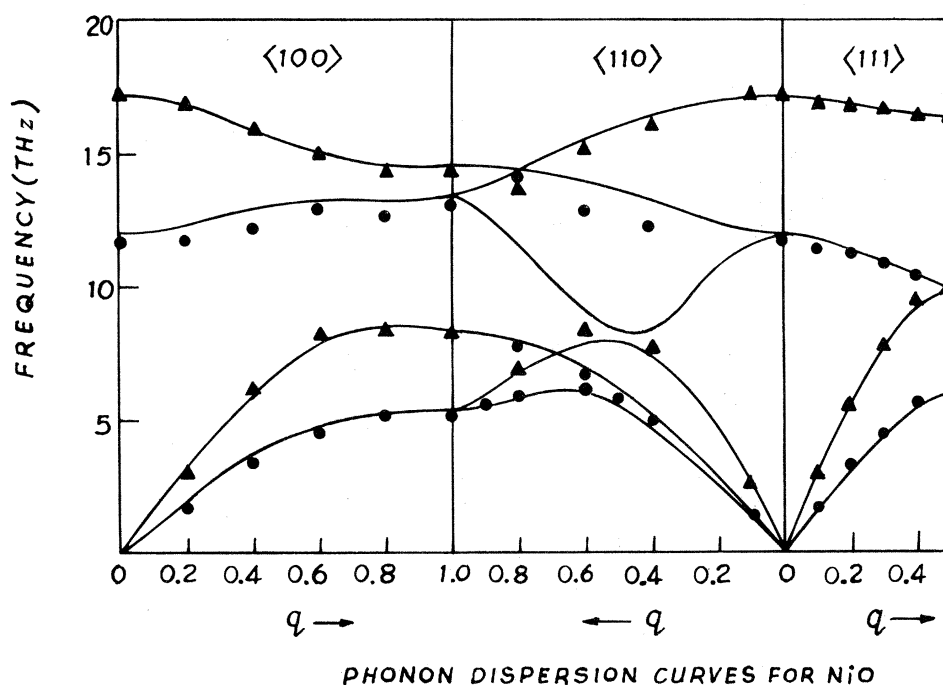

PHONON DISPERSION CURVES FOR NiO

FIG. 1. Solid lines show dispersion curves of NiO calculated from the present model; experimental points are taken from Ref. 12.

TABLE IV. Dielectric properties.

Property	Calculated by Reichardt[a]	Present calculation	Expt.[a]
ϵ_∞	5.7	5.7	5.7
ϵ_0	13.0	11.75	11.75
ω_{TO}	71.94×10^{12}	75.40×10^{12}	72.88
ω_{LO}	103.29×10^{12}	108.26×10^{12}	108.70

[a]Reference 12.

IV. LATTICE DYNAMICAL AND DIELECTRIC PROPERTIES

The dynamical equations are obtained by the usual procedure by expanding Eqs. (6) and (7) about the equilibrium configuration (see Ghosh et al.[6]):

$$[(Z+D)c(Z+D^T)+R'+Q^{(1)}]U$$

$$+[(Z+D)c-R'\mu_0^{-1}+Q^{(2)}]\mu = \omega^2 mU , \tag{13}$$

$$[-c(Z+D^T)-\mu_0^{-1}R'+Q^{(2)}]U$$

$$+[c+\alpha^{-1}+\mu_0^{-1}R'\mu_0^{-1}]\mu = 0 ,$$

where Z, μ_0 and m are the usual 6×6 diagonal matrices and $U = (U_1, U_2)$ and $\mu = (\mu_1, \mu_2)$ are the ionic-displacement and dipole-fluctuation vectors. The matrix R' is given by

$$R' = R + H + V + T + M , \tag{14}$$

where R, H, V, T, and M represent the NN overlap, O^{2-}-O^{2-} overlap, the van der Waals, the three-body, and the magnetic-interaction matrices, where R, H, V, T, and M represent the NN overlap, O^{2-}-O^{2-} overlap, the van der Waals, the three-body, and the magnetic-interaction matrices, respectively. The deformation-dipole matrix $D(ij)$ is defined as follows (see Ref. 6):

$$\vec{\mu}_i^d = \sum_{j \text{ NN of } i} D(ji)U_j = -\sum_{ij'} m_i(r_{ij})\frac{\vec{r}_{ij}}{r_{ij}} .$$

$D(ij)$ involves two parameters m_k and m_k. Here we set $m_k = ce^{-r/\rho'}$ and calculate parameters c and ρ'. Equations (13) have been solved in the symmetry directions to give the phonon frequencies which are shown in Fig. 1. The dielectric equations are the same as given in Ref. 4. The results of our calculation are shown in Table IV.

V. SPIN-WAVE DISPERSION AND MAGNETIC PROPERTIES

Our main intention in this section is to investigate how far the different magnetic properties, in particular the spin-wave dispersion relation in the symmetry directions, are reproducible with the set of parameters which give a more or less satisfactory description of the mechanical properties. We shall treat the Ni^{2+} ions in NiO in the weak-field approximation. We also neglect the slight distor-
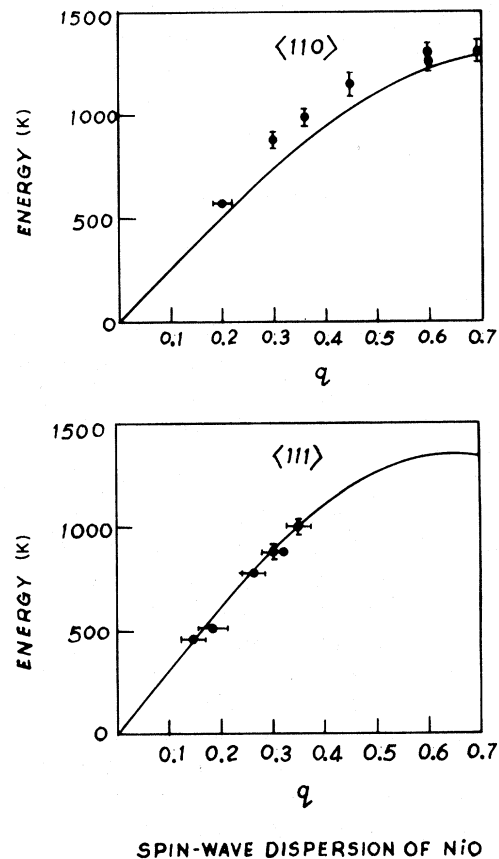

SPIN-WAVE DISPERSION OF NiO

FIG. 2. Solid lines show calculated spin-wave dispersion curves; experimental points are taken from Ref. 16.

tion in structure and treat the lattice in the antiferromagnetic phase as pseudocubic. So, in the present phenomenological spin-wave model the Hamiltonian may be written for a given domain with $S=1$ as

$$H = H_{ex} + H_{anis} ,$$ (15a)

where

$$H_{ex} = \sum_j \sum_{\langle i, \delta_j \rangle} J_j \vec{S}_i \cdot \vec{S}_{i+\delta_j}$$ (15b)

and

$$H_{anis} = \sum_i D_1 (S_i^x)^2 + \sum_i D_2 (S_i^y)^2 .$$ (15c)

In the above expression Z lies along the spin direction and x is at right angles to the ordering plane. $\langle i, \delta_j \rangle$ indicates the summation over the distinct pairs of ions at $\vec{r}_i$ and $\vec{r}_i \mp \delta_j$ coupled through an exchange interaction. Various theoretical and experimental estimates show that in the case of NiO $|J_2| >> |J_1|$. Since other exchanges are smaller than $|J_1|$ we neglect all of them. Similarly the anisotropic terms $(D'S)$ may be disregarded for NiO for all values of the wave vector except for $\vec{q}=0$ for their small size. Brushing aside the finer points which cannot be meaningfully treated in the present crude model, we write below the dispersion relation

$$E_1^2(\vec{q}) = (A_{\vec{q}} - B_{\vec{q}} + D_1)(A_{\vec{q}} + B_{\vec{q}} + D_2)$$ (15d)

$$E_2^2(\vec{q}) = (A_{\vec{q}} - B_{\vec{q}} + D_2)(A_{\vec{q}} + B_{\vec{q}} + D_1) ,$$ (15e)

where $A_{\vec{q}}, B_{\vec{q}}$, and D_1, D_2 are quantities defined in Ref. 16. In this simple model we have only one parameter, namely J_2, which is evaluated from Eqs. (1d) and (5) by using the value of the parameter k^M (180°) given in Table I. Equations (15d) and (15e) are now solved for the symmetry directions to give the magnon frequencies which are shown in Fig. 2. The solid line represents the theoretical calculation, and this is a single curve because in the approximations made, all the curves for the four different domains are degenerate. The experiment also cannot distinguish between them except at $\vec{q}=0$ (not shown in Fig. 2). In view of the drastic approximations made, the agreement is quite satisfactory. This has been possible in the case of NiO because the dominant interaction represented by J_2 is significantly large compared to other relevant interactions. In Table V we compare the value of J_2 obtained in the present calculation with those obtained from different experi-

TABLE V. Comparison of various estimates of $J'S$ (K).

Source	J_1^+	J_1^-	J_2
Neutron diffraction Expt.[a]	−15.7	−16.1	221
Raman scattering Expt.[a]	Small	Small	213
Superexchange[b]	Small	Small	230
Present work	Small	Small	225

[a]Reference 16.
[b]Reference 17.

ments. It is seen that the present estimate of J_2 from the mechanical properties compares quite favorably with the more reliable determination of the same.

Next we calculate some magnetic properties with this value of J_2. We employ the molecular-field theory to estimate these quantities. However, the more accurate random-phase-approximation theory advanced by Lines[19] can also be used. Since the expression for the susceptibility at T_N is the same in both the approaches and the major discrepancies between theory and experiment are similar, we use the simpler molecular-field theory in which the high-temperature expansion of the magnetic susceptibility is given by

$$\chi = \frac{Ng^2\mu_B^2}{\tau}(1 + C_1/\tau + C_2/\tau^2 + \cdots) ,$$ (16a)

where the constants C_1, C_2, and τ are

$$C_1 = \frac{3k\Theta}{S(S+1)} = -6J_2 \text{ and } C_2 = \tfrac{1}{2}C_1^2$$ (16b)

and

$$\tau = \frac{3kT}{S(S+1)} .$$ (16c)

Both the RPA and molecular-field theories envisage

$$\chi(T_N) = Ng^2\mu_B^2/12J_2 ,$$ (17)

and the Néel temperature T_N is given by molecular-field theory

$$T_N = JZS(S+1)/3k .$$ (18)

The calculated values of the above quantities are compared with experiment and more accurate calculations of Hutchings et al.,[16] in Table VI.

TABLE VI. Magnetic properties.

Property	Present	Hutchings et al.[a]	Expt.[a]
Θ (K)	-900	-757	-2000
C_1 (K)	-1350	-1135	
C_2 (K)	9.11×10^5	6.45×10^5	
T_N (K)	900	886	523
$\chi(T_N)$	9.21×10^{-6}	10.1×10^{-6}	11.7×10^{-6}
(emu/gm)			

[a]Reference 16.

VI. DISCUSSION

An examination of the results of the present investigation given in Tables II to VI and Figs. 1 and 2 indicates that the present phenomenological model based on the energy expression (6), where all the terms have some *a priori* justification from microscopic consideration, is capable of giving a rough overall description of both the mechanical and magnetic properties of the NiO crystal with a single set of parameters. Moreover, except for some of the magnetic properties, no large scale discrepancy between calculation and experiment is noticeable anywhere.

Next we discuss some of the major interactions considered whose contributions to the energy are given in Table II. The contribution of the superexchange interaction to the binding energy is quite small but this is indispensable for a simultaneous description of the dispersion of phonons and the elastic properties in the antiferromagnetic phase on one hand, and the dispersion of magnons and the different magnetic properties on the other. Its direct effect on the phonon frequencies is quite small except at very low q values. Hence if one concentrates only on the fit of the phonon frequencies, one is forced to conclude the absence of any sizable magnetic interaction in the antiferromagnetic phase. It is only when we attempt a unified description with a single set of parameters that its importance is clearly demonstrated. Again in view of the fact that the magnon dispersion relation is fairly reproduced, whereas for some of the other magnetic properties the discrepancy is larger, it is reasonable to conclude that it is the molecular-field theory which needs refinement and not the fundamental energy expression used here. This conclu-

sion is because in the derivation of the magnon dispersion relation we have not used the molecular-field theory. However, it should also be noted with Hutchings et al.,[16] that one should be sure of the experimental results in this region before attempting any revision.

Next we find that the quadrupolar interaction which contributes nothing to the cohesive energy is important for producing the lowering of the TO branch particularly in the $\langle 111 \rangle$ direction. Its contribution to the elastic constants is also substantial. Its effect on the TO branch in the $\langle 110 \rangle$ direction is also quite large, being of the order of about 15%. Lastly, the two types of short-range dipolar distortion we have used are necessary for reproducing the dielectric properties, while at the same time keeping the fit for phonons undisturbed. Theoretically there is also no reason to exclude the effect of the first-order exchange interaction while retaining the second-order exchange effects. This point has been discussed in detail in our previous work.[6]

Although we have obtained an overall fit of the different quantities, there still exist some minor discrepancies apart from those in the magnetic properties: The T_1O branch of the phonon-dispersion relation in the $\langle 110 \rangle$ direction near the zone center is about 5% above experiment and there is a somewhat similar discrepancy in the TO branch in the $\langle 100 \rangle$ direction. In the $\langle 110 \rangle$ direction the spin-wave dispersion relation is above experiment between wave vectors $\vec{q} = 0.3$ to $\vec{q} = 0.5$ by about 5 to 10%. In the case of the spin waves it is expected that the inclusion of the exchange interaction other than J_2 will improve the agreement. It is, however, difficult to point out the causes of discrepancy in the phonon dispersion. Further re-

finement might be possible if we can include the small covalency effect the evidence of whose existence is provided by the direct measurement of $\langle S_Z \rangle$ by neutron diffraction experiment.[24]

---

[1]A. Ghosh, A. N. Basu, and S. Sengupta, Proc. R. Soc. London Ser. A **340**, 199 (1974).

[2]A. Ghosh and A. N. Basu, Phys. Rev. B **14**, 4616 (1976).

[3]A. Ghosh and A. N. Basu, Phys. Rev. B **17**, 4558 (1978).

[4]A. N. Basu and S. Sengupta, Phys. Rev. B **14**, 2633 (1976).

[5]A. N. Basu and S. Sengupta, Phys. Status Solidi B **102**, 177 (1980).

[6]S. Ghosh, A. N. Basu, and S. Sengupta, Phys. Rev. B **23**, 1818 (1981).

[7]M. L. Sangster, G. Peckham, and D. H. Saunderson, J. Phys. C **2**, 1026 (1970).

[8]J. Sakurai, W. J. L. Buyers, R. A. Cowley, and G. Dolling, Phys. Rev. **167**, 510 (1968).

[9]B. C. Haywood and M. F. Collins, J. Phys. C **4**, 1299 (1971).

[10]G. Kugel, C. Carabatos, B. Hennion, B. Prevot, and A. Revcolevschi, Phys. Rev. B **16**, 378 (1977).

[11]W. G. Kleppmann and W. Weber, Phys. Rev. B **20**, 1669 (1979).

[12]W. Reichardt, V. Wagner, and W. Kress, J. Phys. C **8**, 3955 (1975).

[13]H. Bilz, M. Buchanan, K. Fischer, and R. Haberkorn, Solid State Commun. **16**, 1023 (1975).

[14]P. de V. Du Plessis, S. J. Van Tonder, and L. Alberts, J. Phys. C **4**, 1983 (1971).

[15]K. S. Aleksandrov, L. A. Shabanova, and L. M. Reshchikova, Fiz. Tverd. Tela (Leningrad) **10**, 1666 1968 [Sov. Phys.—Solid State **10**, 1316 (1968)].

[16]M. T. Hutchings and E. J. Samuelson, Phys. Rev. B **6**, 3447 (1972).

[17]P. W. Anderson, Phys. Rev. **115**, 2 (1959).

[18]P. W. Anderson, in *Solid State Physics*, edited by F. Seitz and D. Turnbull (Academic, New York, 1963), Vol. 14, p. 99.

[19]M. E. Lines and E. D. Jones, Phys. Rev. **141**, 525 (1966).

[20]K. C. Johnson and A. J. Sievers, Phys. Rev. B **10**, 1027 (1974).

[21]H. G. Drickamer, J. Chem. Phys. **47**, 1880 (1967).

[22]S. Ghosh, A. N. Basu, and S. Sengupta, Phys. Status Solidi B **103**, 595 (1981).

[23]J. Owen and J. H. M. Thornley, Rep. Prog. Phys. **29**, Part II, 675 (1966).

[24]M. T. Hutchings and H. J. Guggenheim, J. Phys. C **3**, 1303 (1970).

[25]Ram Pal Singh, G. G. Agrawal, and Jai Shanker, Solid State Commun. **25**, 173 (1978).

[26]F. Seitz, *The Modern Theory of Solids* (McGraw-Hill, New York, 1940).